MS-CASPT2 Calculation of Excess Electron Transfer in Stacked DNA Nucleobases

Lluís Blancafort*,† and Alexander A. Voityuk*,†,‡

Institut de Química Computational, Departament de Química, Universitat de Girona, 17071 Girona, Spain, and Institució Catalana de Recerca i Estudis Avançats, Barcelona 08010, Spain

Received: November 28, 2006; In Final Form: March 12, 2007

Calculations using the complete active space self-consistent field (CASSCF) and complete active space second-order perturbation (CASPT2) methods, and the multistate formulation of CASPT2 (MS-CASPT2), are performed for the ground and excited states of radical anions consisting of two π-stacked nucleobases. The electronic couplings for excess electron transfer (EET) in the π-stacks are estimated by using the generalized Mulliken−Hush approach. We compare results obtained within the different methods with data derived using Koopmans' theorem approximation at the Hartree−Fock level. The results suggest that although the one-electron scheme cannot be applied to calculate electron affinities of nucleobases, it provides reasonable estimates for EET energies. The electronic couplings calculated with KTA lie between the CASPT2 and the MS-CASPT2 based values in almost all cases.

Introduction

The last 15 years have been very important for understanding mechanisms of charge transfer (CT) through DNA π-stacks.[1] There are two types of charge transfer in DNA: (1) positive charge or electron hole transfer (HT) when a radical cation state moves from one base pair to another and (2) excess electron transfer (EET) when a radical anion state migrates through the π-stack. The majority of experimental and theoretical studies of charge transfer in DNA have been related to HT, that is, to the propagation of radical cation states of nucleobases along the duplex. In the past, investigations of excess electron transport were restricted to electron spin resonance.[2] Recently, several photochemical and spectroscopic studies of EET have been published[3−6] (see also references in ref 7). It has been shown that EET has a large potential for nanodevices,[8] in particular, for DNA chip technology.[9] Moreover, electron attachment to DNA may induce strand breaks via dissociative electron attachment[10,11] as well as the splitting of pyrimidine photodimers.[12,13,14] Therefore, computational insight into the mechanistic and dynamic issues of EET in DNA is now of special interest. Elementary steps for charge transfer in DNA and general aspects of charge-transfer modeling have been discussed in the literature (see, for instance, refs 15−20 and references therein).

The ability of DNA to mediate an excess electron is associated with the formation of radical anion states of nucleobases. Two types of radical anion states of nucleobases exist: (1) dipole-bound anions where the excess electron is located far outside the molecule[21−25] and (2) valence (covalently bound) anionic states where the electron is delocalized over the molecule. In the gas phase, the nucleobase anions may be described as electron-dipole-bound states.[26−28] However, it has been shown that hydrogen bonds between an anion and its surroundings stabilize the valence-bound state.[26−28] The energetics and structure of radical anion states of nucleobases and their complexes have been intensively studied theoretically.[29−34] The quantum-mechanical treatment of radical anion states of nucleobases and their complexes needed to model EET is more complicated[28−34] than the calculations of radical cation states in the case of HT.

In a DNA π-stack, where donor and acceptor are separated by one or more intervening base pairs, EET is expected to fall well within the nonadiabatic regime,[35] and therefore, the rate of electron transfer is proportional to the square of electronic coupling V_{da} between the donor and acceptor sites.[36,37] Thus, the electronic coupling is a key characteristic which controls the rate of charge transfer and determines its sensitivity to the arrangement of the donor and acceptor. There are several computational studies of electronic couplings for hole transfer in DNA.[16,19,38−40] In most studies, Koopmans' theorem approximation (KTA) has been used to calculate the HT couplings.[19,38−40] While KTA has proven to be quite acceptable for the treatment of radical cations, this approximation is more limited when modeling negatively charged systems. The reason for this limitation is well-known. By detaching an electron from a neutral system, the electronic relaxation and changes in the correlation energy are of opposite sign and partially cancel each other, while these terms are of the same sign when an excess electron is attached to the system.

However, in EET, one is primarily interested in the energy difference between the states involved in the process rather than in the absolute energy of the electron attachment. When an excess electron moves in DNA from one nucleobase to another, the relevant states are of the same nature, and therefore, the reorganization and correlation effects for these states should be similar and cancel out. Because of this, we expect that the one-electron approximation (i.e., KTA) may give reasonable estimates for EET energetics in spite of its failure to predict the electron affinity. Within the KTA scheme, the properties of adiabatic states of a radical anion can be approximately estimated using the lowest unoccupied molecular orbitals (LUMOs) of the corresponding neutral system. Recently, an efficient approach has been considered for calculating electronic couplings for EET in DNA π-stacks.[35] The good agreement

* E-mail: lluis.blancafort@udg.es (L. B.); alexander.voityuk@icrea.es (A. V.).
† Universitat de Girona.
‡ Institució Catalana de Recerca i Estudis Avançats.

10.1021/jp067886z CCC: $37.00
Published on Web 05/08/2007

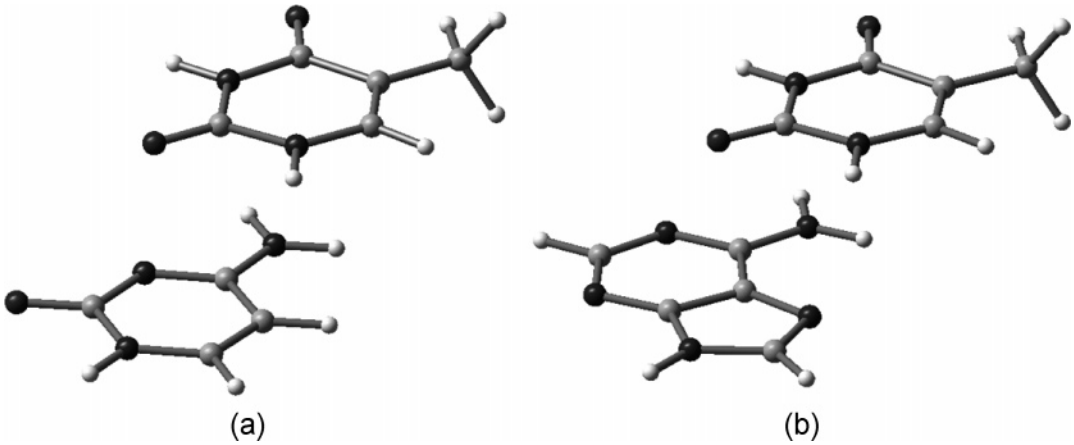

Figure 1. Representative structures of stacked base pairs. (a) TC. (b) TA.

between matrix elements obtained within the diabatic state method for radical anion systems with the corresponding estimates derived from KTA allows one to conclude that reasonable values of EET couplings can be obtained by using LUMOs of isolated neutral base stacks calculated without diffuse functions. When, however, the diffuse functions are added to the basis set, the LUMOs exhibit the dipole-bound character and cannot be employed for computing the coupling matrix elements.[35] However, the question about the role of electron correlation in the calculation of EET parameters still remains.

The purpose of this paper is to calculate the EET matrix elements beyond the one-electron approximation and to study how important the electron-correlation effects are on the coupling in negatively charged DNA π-stacks (see Figure 1 for examples of the stacked structures). Recently, we have carried out calculations of the electronic couplings for hole transfer using multireferential methods.[41] The computational results of that study have been used as benchmarks for estimating the accuracy of the time-dependent density functional theory (DFT) approach[42] and for assessment of semiempirical methods.[43] Here, we have used the same methods (complete active space self-consistent field, CASSCF; complete active space second-order perturbation, CASPT2; and multistate CASPT2, MS-CASPT2) for the calculation of electronic coupling in single-strand DNA stacks consisting of two nucleobases. Using the generalized Marcus−Hush (GMH) approach, the couplings are obtained from the excitation energies and the transition dipole moments. Here, we use the CAS-PT2 or MS-CASPT2 excitation energies, which include dynamic correlation. For the dipole moments, we use the CASSCF wave function, or the perturbatively modified complete active space configuration interaction (PM-CASCI) wave function derived from the MS-CASPT2 calculations. The MS-CASPT2 based dipole moments are substantially different from the CASSCF ones, and the results could not be converged. Thus, the calculated couplings cannot be considered as benchmarks, but the present results determine their boundaries, within the limitations of the 6-311G* basis set. In most cases, the coupling elements obtained with KTA lie inside these boundaries, suggesting the usefulness of KTA to estimate electronic couplings for EET.

Computational Details

CASSCF Calculations. The CASSCF calculations are carried out for several one-strand DNA stacks consisting of two nucleobases using the standard 6-311G* basis set and the program Gaussian03.[44] For the CASSCF calculations, active spaces of 13 electrons in 12 orbitals (six orbitals per nucleobase), (13,12), were used following the strategy outlined in our previous paper on radical cations of similar systems.[41] The energies of the ground and excited states are obtained from a single calculation, using state-averaged orbitals with equal weights for each state. The dipole moments of each state and the transition dipole moments between the two states are derived from the same calculation. For a better estimation of the dimer properties (energies, dipoles, and transition dipole moments), these are recalculated with the program MOLCAS 5.4[45] at the CASPT2 and MS-CASPT2 levels (multistate formulation of CASPT2 which accounts for the nonorthogonality of the CASPT2 wave function),[46] with a real level shift parameter of 0.3. Using this parameter, the weights of the CASSCF reference function in the CASPT2 functions of the ground and excited states differed by 0.001 or less in all cases. For the transition dipole moments, the values reported as MS-CASPT2 are the ones obtained from the PM-CASCI wave function.[46]

The values of the off-diagonal elements of the MS-CASPT2 effective Hamiltonian, which are indicative of the reliability of the MS-CASPT2 results,[47] are presented in the Supporting Information (Table SI1). The averages and differences of the off-diagonal elements ($|H_{12} + H_{21}|/2$ and $|H_{12} - H_{21}|$, respectively) are smaller than 2 kcal mol^{-1} (0.09 eV) in all cases except CT and TC, with a maximal value of 0.17 eV. In relative terms, the value of ($|H_{12} + H_{21}|/2$) is smaller than 10% of the CASPT2 energy gap ($H_{22} - H_{11}$) in all cases except CT, TC, and AT.

The ground-state charge distribution on the dimers presented in Table 1 (q_X and q_Y) is obtained from the Mulliken charges except for the MS-CASPT2 values, which are obtained from the dipole moments. Thus, for radical anion dimers 5′-XY-3′ with *z*-orientation (the plane of each nucleobase is perpendicular to *z*-axis), and the 5′-X nucleobase lying in the *xy* plane:

$$q_X = -1 - \frac{\mu_z}{4.803 \times r} \qquad q_Y = -1 - q_Y \tag{1}$$

where q_X and q_Y are charges on fragments X and Y in au, r is the distance (in Å) between nucleobase planes ($r = 3.38$ Å in the systems under study), and μ_z is the *z*-component of the dipole moment in the stack (in Debye). To prove that both schemes provide almost identical values, we have recalculated the CASSCF charge distribution using eq 1. The dipole-based estimates deviate by 2% or less from the Mulliken charges.

The electron affinities of the nucleobases have been calculated at the CASSCF/6-311G* and CASPT2/6-311G* levels of theory (real level shift 0.3), with the purpose of estimating the relative

TABLE 1: Excitation Energy (ΔE_{12}), Transition Dipole Moment (μ_{12}), Electronic Coupling V, and Charge on Nucleobase X (q_X) and Y (q_Y) in 5′-XY-3′ in Dimers Calculated with CASSCF (in Short, CAS), CASPT2, MS-CASPT2 (in Short, MS-PT2), and KTA

XY	method	ΔE_{12}, eV	$\Delta\mu$, D	$\lvert\mu_{12}\rvert$, D	$\lvert V\rvert$, eV	q_X	q_Y
TT	CAS	0.157	−15.846	0.370	0.367E-02	−0.981	−0.019
	CASPT2	0.155			0.362E-02	−0.986	−0.014
	MS-PT2	0.155	−15.804	0.686	0.670E-02	−0.980	−0.020
	KTA	0.193	−15.466	1.141	0.141E-01	−0.971	−0.029
T_T	CAS	0.011	32.444	0.017	0.576E-05	−0.001	−0.999
	CASPT2	0.018			0.943E-06	+0.003	−1.003
	MS-PT2	0.018	32.445	0.010	0.554E-05	−0.001	−0.999
	KTA	0.022	32.474	0.011	0.745E-05	−0.000	−1.000
CT	CAS	0.349	−14.381	3.247	0.718E-01	−0.929	−0.071
	CASPT2	0.067			0.138E-01	−0.935	−0.065
	MS-PT2	0.098	−5.117	7.463	0.464E-01	−0.643	−0.357
	KTA	0.119	−3.637	7.630	0.578E-01	−0.620	0.380
TC	CAS	0.178	−8.342	6.790	0.758E-01	−0.753	−0.247
	CASPT2	0.299			0.127E+00	−0.750	−0.250
	MS-PT2	0.401	−15.239	2.328	0.586E-01	−0.966	−0.034
	KTA	0.409	−13.941	3.780	0.975E-01	−0.936	0.064
TA	CAS	0.382	−15.966	0.783	0.186E-01	−0.992	−0.008
	CASPT2	0.435			0.212E-01	−0.983	−0.017
	MS-PT2	0.435	−16.018	0.438	0.119E-01	−0.994	−0.006
	KTA	0.668	−15.945	0.508	0.212E-01	−0.995	−0.005
AT	CAS	0.372	14.962	2.561	0.602E-01	−0.040	−0.960
	CASPT2	0.486			0.787E-01	−0.046	−0.954
	MS-PT2	0.504	15.784	0.468	0.149E-01	−0.014	−0.986
	KTA	0.660	15.461	1.039	0.440E-01	−0.028	−0.972
TG	CAS	0.259	−15.579	2.061	0.331E-01	−0.998	−0.002
	CASPT2	0.581			0.743E-01	−0.975	−0.025
	MS-PT2	0.590	−16.066	0.620	0.227E-01	−1.013	+0.013
	KTA	0.818	−16.044	0.923	0.468E-01	−0.995	−0.005
GT	CAS	0.760	15.094	2.286	0.110E+00	−0.040	−0.960
	CASPT2	1.043			0.151E+00	−0.042	−0.958
	MS-PT2	1.054	15.581	1.223	0.817E-01	−0.025	−0.975
	KTA	1.308	15.031	1.593	0.136E+00	−0.027	−0.973

diabatic energies of the donor and acceptor states with the two methods. The electron affinity is calculated as the energy difference between the neutral species and the radical anion, using (6,6) and (7,6) active spaces, respectively. The results are presented in Table SI2 (Supporting Information). Overall, the electron affinity of thymine is underestimated with respect to the remaining three bases at the CASSCF level, when compared with CASPT2.

KTA Calculations. The KTA values are based on Hartree−Fock (HF) calculations of neutral stacks performed using the standard 6-31G* basis for consistency with the previous study.[35] For the systems considered, we have always used unoccupied molecular orbitals (MOs) corresponding to "+" and "−" combinations of donor and acceptor orbitals (π^* orbitals of nucleobases). They correspond to LUMO and LUMO+1. In similar calculations (e.g., with another basis set or for other geometries), LUMO or LUMO+1 may correspond to σ^* orbitals. In such cases, other virtual states (LUMO+i, LUMO+j) should be employed.

Estimation of Electronic Couplings. The generalized Mulliken−Hush (GMH) method introduced by Cave and Newton was employed to calculate electronic couplings.[48,49]

Within the two-state GMH model,[48,49] the electronic coupling can be expressed via the vertical excitation energy $\Delta E_{12} = E_2 - E_1$, the difference between the adiabatic dipole moments $\Delta\mu = \mu_2 - \mu_1$, and the transition dipole moment μ_{12}:

$$V_{da} = \frac{\Delta E_{12}|\mu_{12}|}{\sqrt{\Delta\mu^2 + 4\mu_{12}^2}} \qquad (2)$$

The details of calculation are considered in our previous paper.[41] In particular, we have used $\Delta\mu^z$ and μ_{12}^z, that is, the projections of the dipole moments along the z-axis; the z superscript has been dropped for simplicity. The V_{da} listed in Table 1 is obtained as follows: CASSCF couplings from CASSCF energies and dipole moments, CASPT2 values from CASPT2 energies and CASSCF dipole moments, MS-CASPT2 values from MS-CASPT2 energies and PM-CASCI dipole moments, and KTA couplings from the energy differences and dipole moment matrix elements calculated with the relevant orbitals of the neutral stacks.

Geometries. As in our previous study, experimental idealized atomic coordinates of the nucleobases (adenine, cytosine, guanine, and thymine) taken from high-resolution X-ray and neutron studies were used for generating the structures.[50] These structural parameters are nearly always employed to generate DNA models. As already noted, within the KTA scheme, ET properties in radical anion systems are estimated using HF calculations of neutral systems. For the sake of consistency when comparing the calculation results, we employ the same geometries also in the CASSCF and CASPT2 computations of radical anion states.

The mutual positions of the nucleobases in the models studied correspond to a regular B-DNA structure (see Figure 1). The geometries of the systems were constructed with the program SCHNArP.[51]

Results and Discussion

General Remarks. CASSCF and Second-Order Perturbed Results. The electronic characteristics of dimers calculated using CASSCF, CASPT2, MS-CASPT2, and KTA are listed in Table 1. Our general approach is to include nondynamic correlation at the CASSCF level and dynamic correlation with second-order perturbation. For the energy, this is achieved with the CASPT2

method. The effect of dynamic correlation can be explained on the basis of the relative electron affinities of the isolated nucleobases (see Table SI2, Supporting Information), calculated at the CASSCF and CASPT2 levels. Although the electron affinities themselves are not accurate, their relative values can be used as estimates of the diabatic energies of donor and acceptor, in the frame of a two-state model for EET (in this case, neglecting electrostatic effects of the neighboring base). Thus, the electron affinities of A, C, and G are shifted downward with respect to T at the CASPT2 level. This implies that the diabatic energies of A, C, and G are increased with respect to T upon inclusion of dynamic correlation. As a consequence, the excitation energies for TX and XT pairs (X = A, C, or G), where T is the donor, are increased at the CASPT2 and MS-CASPT2 level with respect to the CASSCF values. The only exception to this trend is CT. Here, the CASPT2 excitation energy is lower than the CASSCF one because T is the acceptor due to electrostatic conformational effects.

The changes in the diabatic energies also affect the charge distribution and the transition dipole moments. Thus, within a two-state model, the excess charge distribution, expressed as the difference of charges on donor and acceptor ($\Delta q = q_Y - q_X$), is determined by the difference of the diabatic energies of the donor and acceptor ($\Delta\epsilon = \epsilon_Y - \epsilon_X$) and the electronic coupling V of the sites (see refs 37 and 52 for details):

$$\Delta q = \frac{\Delta\epsilon}{\sqrt{\Delta\epsilon^2 + 4V^2}} \tag{3}$$

Here, $\Delta\epsilon$ can be approximated by the difference of electron affinities of the X and Y nucleobases. Because the electronic coupling of neighboring nucleobases is rather weak ($V \sim 0.1$ eV), the differences in $\Delta\epsilon$ within the CASSCF and CASPT2 schemes must lead to redistribution of the excess charge in the stack. This has motivated us to recompute the dipole moments $\Delta\mu$ and μ_{12} with the PM-CASCI wave function obtained from the MS-CASPT2 treatment. However, the MS-CASPT2 results are only reliable when the multistate correction is small. This can be estimated on the basis of the off-diagonal elements of the MS-CASPT2 effective Hamiltonian (see Table SI1, Supporting Information). It has been suggested that reliable MS-CASPT2 results are obtained when the off-diagonal elements are below a threshold of 2 kcal mol^{-1} (0.09 eV).[47] This condition is fulfilled for all the stacked pairs described here except for CT and TC, where the off-diagonal elements reach up to 5 kcal mol^{-1} (0.22 eV). Still, there are substantial differences between the transition dipole moments μ_{12} calculated at the CASSCF level and the MS-CASPT2 based values and also for the cases where the coupling is small. This can be understood taking into account that dynamic correlation induces a change in the charge distribution (through $\Delta\epsilon$) which results in a change in $\Delta\mu$. At the same time, the sum $(\Delta\mu)^2 + 4(\mu_{12})^2$ for the CASSCF and PM-CASCI dipole moments is the same. Thus, the PM-CASCI wave functions Ψ_k are linear combinations of the two lowest CASSCF eigenfunctions Φ_i.[46]

$$\Psi_k = \sum_{i=1,2} c_{ki}\Phi_i$$

The dipole moments are elements of the matrix obtained from the $\{\Phi_i\}$ or $\{\Psi_i\}$ sets and the dipole moment operator (of dimension 2×2 in the present case). Since the transformation between the two sets is unitary (the coefficients c_{ki} are the eigenvectors of the symmetrized MS-CASPT2 Hamiltonian), the matrices evaluated with either basis have the same eigenvalues $(\mu_{11} + \mu_{22})/2 \pm (1/2)\sqrt{(\Delta\mu)^2 + 4(\mu_{12})^2}$ and the same trace $\mu_{11} + \mu_{22}$. Thus, the sum of $(\Delta\mu)^2 + 4(\mu_{12})^2$ evaluated with either set of wave functions (CASSCF or PM-CASCI) is the same. Because of the relative magnitudes of $\Delta\mu$ and μ_{12}, small relative changes in $\Delta\mu$ result in large relative changes in μ_{12}.

Excess Charge Distribution in Dimers. The excess charge distribution in the ground state predicted by the KTA and multireference approaches is in good agreement for all cases except for CT and TC. Thus, the localization of the charge is the result of two effects, the difference in electron affinities of nucleobases and the preference for charge localization on the 5′ end (because of electrostatic interactions of the bases which in turn depend on the orientation of the nucleobases). Following the larger electron affinity of T, in the pairs with A or G the excess electron in the ground state is more than 95% localized on T, irrespective of its position (5′ or 3′ end). However, the preference of the 5′ end for negative charge localization[53] is reflected in the fact that the amount of charge localized on the purine is larger for the AT and GT than for the TA and TG pairs. For the same reason, in the TT pair, the ground-state charge is almost completely localized on the 5′ end. In the T_T case, however, the conformational effect is different and the charge is localized on the 3′ end. Ideally, the calculated charges on each nucleobase should not be smaller than −1. In a few cases, the values are smaller than that (with a net positive charge on the complementary base), but the effects are small (less than 0.02 electron).

Let us now consider the charge delocalization in CT and TC. In general, it is accepted that T has a larger electron affinity than C, and one would expect charge localization on T to be preferred. However, for CT there is net charge localization on 5′-C because of the electrostatic interactions. In contrast to this, the charge in TC is localized on 5′-T. Although all methods predict localization of the charges on the same base of each pair, there are substantial quantitative differences between CASSCF and MS-CASPT2. Thus, the CASSCF(13,12) calculations predict almost complete (>90%) charge localization on C for CT, with more significant delocalization (approximately 25%) in TC. The Mulliken charges for the CASPT2 wave function give similar values. In contrast to this, the KTA and MS-CASPT2 based values predict only partial localization (approximately 60%) on C in CT and almost complete localization (>90%) on T in TC. The changes are due to the small difference between the diabatic energies of the two pyrimidine bases. Thus, small changes in $\Delta\epsilon$ (eq 3) have a large effect on the charge distribution. In any case, one can expect that the effects of polar environment should essentially suppress the negative charge delocalization in DNA leading to radical anion states confined to single pyrimidine sites, in line with the conclusion derived for the hole delocalization.[54]

The calculated ground- and excited-state charge distributions are in agreement with the two-state model. According to this model, the charges on the donor and acceptor should be exchanged when going from the ground to the excited state. Thus, in the lowest excited state of the purine−thymine dimers, the negative charge is transferred from T to the purine base, whereas in the excited state of TT, TC, and CT dimers the excess charge is mainly localized on the 3′-side nucleobase. Overall, in the two-state model the sum of the ground- and excited-state charges on the same fragment should be equal to 1, and the sum of the calculated MS-CASPT2 and CASSCF charges for all cases differs by less than 0.04 electron from the ideal value.

Excitation Energies. The dimers TT and T_T formed by thymine bases differ in the arrangement of nucleobases. While

in the TT stack the thymines are at the distance 3.38 Å, the T_T complex was obtained by removing the bridging nucleobase B from a TBT trimer of the regular structure; the distance between thymine bases is 6.76 Å. The energy gap (ΔE_{12}) in TT ranges from 0.15 to 0.20 eV depending on the calculation method. This gap is mainly due to the electrostatic interactions between the bases. The contribution of covalent interaction (electronic coupling) to the splitting is essentially smaller. Increasing the separation between thymines (by going from TT to T_T) leads to a remarkable decrease in the gap, which is 0.01−0.02 eV. Because C and T have similar electron affinities, one expects the gap in the dimers CT and TC to be as large as in TT. The CASPT2 and MS-CASPT2 calculations predict that ΔE_{12} in CT is of ∼0.1 eV while in TC it is of 0.3−0.4 eV, and the KTA values are in agreement with that. Thus, the energy gap is quite sensitive to conformational changes in the dimers, as CT and TC differ from each other solely by the twist angle. As expected from the larger electron affinity of T, the energy gaps for the dimers of T and a purine are larger than 0.4 eV. In this context, by passing from TA to AT, ΔE_{12} does not change much while the energy gap in TG is remarkably smaller than that of GT. This difference is due to a larger dipole moment of G as compared to A.

Overall, the comparison of ΔE_{12} of the pyrimidine dimers calculated at the different levels of theory suggests that KTA estimates are in good agreement with the CAS-PT2 and MS-CASPT2 results. In contrast to this, KTA overestimates the energy gaps for the dimers formed by T and a purine base by about 30%.

Transition Dipole Moments and Coupling Elements. The transition dipole moments are particularly sensitive to changes in charge distribution. This explains the large differences between the values obtained with different methods. Thus, the MS-CASPT2 based values of μ_{12} differ by up to a factor of 5.4 with respect to the CASSCF based values. However, as we have argued above, the changes are physically reasonable, at least from a qualitative point of view, as they are due to shifts in the diabatic energies in the right direction. In principle, the MS-CASPT2 based values could be refined by enlarging the CASSCF active space until convergence of the CASSCF and MS-CASPT2 based dipole moments. This strategy is not feasible presently because of computational limitations, but the "converged" MS-CASPT2/6-311G* result must lie between the CASSCF and MS-CASPT2 based dipole moments. For most cases, the values of μ_{12} obtained with KTA lie between these boundaries.

The differences in μ_{12} on the basis of the different methods give rise to similar differences in the couplings. However, all methods give the same order of magnitude for the couplings in each stacked pair.

Conclusions

The excitation energies, dipole moments, and electronic coupling elements V_{12} for EET have been calculated at the multireferential level, using the CASSCF, CASPT2, and MS-CASPT2 approaches. The results depend on the level of theory. Therefore, dynamic correlation should be taken into account for a correct estimation of the coupling elements and energetics of EET. In the present study, this has been done by calculating the excitation energies at the CASPT2 and MS-CASPT2 levels of theory and by calculating the dipole moments from the PM-CASCI wave function obtained with MS-CASPT2.

Because the multistate interaction for several systems (CT, TC, and AT, see Computational Details) is found to be not small, the MS-CASPT2 method cannot provide very accurate results for these systems. Enlarging the CASSCF active space until the CASSCF and MS-CASPT2 based values of μ_{12} are converged is required to obtain the benchmark values which must lie between the CASPT2 and MS-CASPT2 based values of Table 1.

We have compared results obtained within the accurate methods with data derived using KTA at the Hartree−Fock level. The comparison suggests that although the one-electron scheme cannot be applied to calculate electron affinities of nucleobases, it provides reasonable estimates for EET energies. The electronic couplings calculated with KTA lie between the CASPT2 and the MS-CASPT2 based values in almost all cases.

Our results show that the excess electron in isolated dimers is largely localized on a single base. Because embedding any system into a polar environment should confine the excess charge, we expect that an excess electron in DNA will be confined to single pyrimidines but not be delocalized over several nucleobases.

Acknowledgment. This work has been supported Project No. CTQ2005-04563 of the Spanish Ministerio de Educación y Ciencia (MEC), the Ramón y Cajal program of the MEC (fellowship for L. B.), the European COST Action P9 "Radiation Damage in Biomolecular Systems", and a grant from the Francesca Roviralta Foundation. The use of the computational facilities of the Catalonia Supercomputer Center (CESCA) is also gratefully acknowledged.

Supporting Information Available: Tables SI1 (off-diagonal elements of the MS-CASPT2 effective Hamiltonian) and SI2 (relative CASSCF and CASPT2 electron affinities of isolated nucleobases); complete ref 44 and 45; and Cartesian coordinates for the dimer stacks. This material is available free of charge via the Internet at http://pubs.acs.org.

References and Notes

(1) *Long-Range Charge Transfer in DNA. Topics in Current Chemistry*; Shuster, G. B., Ed.; Springer: Berlin, 2004; Vol. 236, 237.
(2) Cai, Z.; Sevilla, M. D. *Top. Curr. Chem.* **2004**, *237*, 103−127.
(3) Lewis, F. D.; Liu, X.; Miller, S. E.; Hayes, R. T.; Wasielewski, M. R. *J. Am. Chem. Soc.* **2002**, *124*, 11280.
(4) Giese, B.; Carl, B.; Carl, T.; Carell, T.; Behrens, C.; Hennecke, U.; Schiemann, O.; Feresin, E. *Angew. Chem., Int. Ed.* **2004**, *43*, 1848.
(5) Ito, T.; Rokita, S. E. *Angew. Chem., Int. Ed.* **2004**, *43*, 1839.
(6) Kaden, P.; Mayer-Enthart, E.; Trifonov, A.; Fiebig, T.; Wagenknecht, H.-A. *Angew. Chem., Int. Ed.* **2005**, *44*, 1636.
(7) Wagenknecht, H. A. *Angew. Chem., Int. Ed.* **2003**, *42*, 2454.
(8) Park, S. J.; Taton, T. A.; Mirkin, C. A. *Science* **2002**, *295*, 1503.
(9) Boon, E. M.; Salas, J. E.; Barton, J. K. *Nat. Biotechnol.* **2002**, *20*, 28.
(10) Zheng, Y.; Cloutier, P.; Hunting, D.; Wagner, J. R.; Sanche, L. *J. Am. Chem. Soc.* **2004**, *126*, 1002.
(11) Simons, P. *Acc. Chem. Rev.* **2006**, *39*, 772.
(12) Voityuk, A. A.; Michel-Beyerle, M. E., Rösch, N. *J. Am. Chem. Soc.* **1996,** *118*, 9750.
(13) Harrison, C. B.; O'Neil, L. L.; Wiest, O. *J. Phys. Chem. A* **2005**, *109*, 7001.
(14) Zhang, R. B.; Eriksson, L. A. *J. Phys. Chem. B* **2006**, *110*, 7556.
(15) Jortner, J.; Bixon, M.; Voityuk, A. A.; Rösch, N. *J. Phys. Chem. A* **2002**, *106*, 7599.
(16) Berlin, Y. A.; Kurnikov, I. V.; Beratan, D. N.; Ratner, M. A.; Burin, A. L. *Top. Curr. Chem.* **2004**, *237*, 1−36.
(17) Senthilkumar, K.; Grozema, F. C.; Guerra, C. F.; Bickelhaupt, F. M.; Lewis, F. D.; Berlin, Y. A.; Ratner, M. A.; Siebbeles, L. D. A. *J. Am. Chem. Soc.* **2005**, *127*, 14894.
(18) Berlin, Y. A.; Burin, A. L.; Ratner, M. A. *Chem. Phys.* **2002**, *275*, 61.
(19) Tong, G. S. M.; Kurnikov, I. V.; Beratan, D. N. *J. Phys. Chem. B* **2002**, *106*, 2381.
(20) Voityuk, A. A. In *Computational studies of DNA and RNA*; Šponer, J., Lankas, F., Eds.; Springer: Dordrecht, 2006; pp 485−512.

(21) Oyler, N. A.; Adamowicz, L. *Chem. Phys. Lett.* **1994**, *219*, 22.
(22) Adamowicz, L. *J. Phys. Chem.* **1993**, *97*, 11122.
(23) Desfrançois, C.; Abdoul-Carime, H.; Schermann, J. P. *J. Chem. Phys.* **1996**, *102*, 7792.
(24) Hendricks, J. H.; Lyapustina, S. A.; de Clercq, H. L.; Snodgrass, J. T.; Bowen, K. H. *J. Chem. Phys.* **1996**, *104*, 7788.
(25) Hendricks, J. H.; Lyapustina, S. A.; de Clercq, H. L.; Bowen, K. H. *J. Chem. Phys.* **1998**, *108*, 8.
(26) Al-Jihan, I.; Smets, J.; Adamowicz, L. *J. Phys. Chem. A* **2000,** *104*, 2994.
(27) Adamowicz, L. *J. Phys. Chem.* **1996**, *100*, 14655.
(28) Smith, D. M.; Elkady, Y.; Adamowicz, L. *J. Phys. Chem. A* **1999**, *103*, 4404, 5784.
(29) Sevilla, M. D.; Besler, B.; Colson, A.-O. *J. Phys. Chem.* **1995**, *99*, 1060.
(30) Li, X.; Sevilla, M. D. *J. Phys. Chem. A* **2002**, *106*, 1596.
(31) Russo, N.; Toscano, M.; Grand, A. *J. Comput. Chem.* **2002**, *14*, 1243.
(32) Richardson, N. A.; Wesolowski, S. S.; Schaefer, H. F., III. *J. Am. Chem. Soc.* **2002**, *124*, 10163.
(33) Richardson, N. A.; Wesolowski, S. S.; Schaefer, H. F., III. *J. Phys. Chem. B* **2003**, *107*, 848.
(34) Haranczyk, M.; Gutowski, M. *J. Am. Chem. Soc.* **2005**, *127*, 699.
(35) Voityuk, A. A. *J. Chem. Phys.* **2005**, *123*, 034903.
(36) Marcus, R. A.; Sutin, N. *Biochim. Biophys. Acta* **1985**, *811*, 265.
(37) Newton, M. D. *Chem. Rev.* **1991**, *91*, 767.
(38) Voityuk, A. A.; Bixon, M.; Jortner, J.; Rösch, N. *J. Chem. Phys.* **2001**, *114*, 5614.
(39) Voityuk, A. A.; Rösch, N.; Bixon, M.; Jortner, J. *J. Phys. Chem. B* **2000**, *104*, 9740.
(40) Rösch, N.; Voityuk, A. A. *Top. Curr. Chem.* **2004**, *237*, 37−72.
(41) Blancafort, L.; Voityuk A. A. *J. Phys. Chem. A* **2006**, *110*, 6426.
(42) Sevilla, M. D.; Kumar, A. *J. Phys. Chem. B* **2006**, *110*, 24181.
(43) Voityuk, A. A. *Chem. Phys. Lett.* **2006**, *427*, 177.
(44) Frisch, M. J. et al. *Gaussian 03*; Gaussian, Inc.: Pittsburgh, PA, 2003.
(45) Andersson, K. et al. *MOLCAS*, version 5.4; University of Lund: Lund, Sweden, 2003.
(46) Finley, J.; Malmqvist, P.-Å.; Roos, B.; Serrano-Andrés, L. *Chem. Phys. Lett.* **1998**, *288*, 299.
(47) Serrano-Andrés, L.; Merchán, M.; Lindh, R. *J. Chem. Phys.* **2005**, *122*, 104107.
(48) Cave, R. J.; Newton, M. D. *J. Chem. Phys.* **1997**, *106*, 9213.
(49) Cave, R. J.; Newton, M. D. *Chem. Phys. Lett.* **1996**, *249*, 15.
(50) Clowney, L.; Jain, S. C.; Srinivasan, A. R.; Westbrook, J.; Olson, W. K.; Berman, H. W. *J. Am. Chem. Soc.* **1996**, *118*, 509.
(51) Lu, X. J.; El Hassan, M. A.; Hunter, C. A. *J. Mol. Biol.* **1997**, *273*, 681.
(52) Voityuk, A. A. *J. Phys. Chem. B* **2005**, *109*, 10793.
(53) Voityuk, A. A.; Michel-Beyerle, M. E.; Rösch, N. *Chem. Phys. Lett.* **2001**, *342*, 231.
(54) Voityuk, A. A. *J. Chem. Phys.* **2005**, *122*, 204904.